Fermilab Library
0 1160 0052443 3

SSC-SDE-27

SSC-SDE
SOLENOIDAL DETECTOR NOTES

ON-CHIP FILTERING OF LOW P_t TRACK WITH STRAW-TUBE CHAMBER
January 16, 1990

Takashi Ohsugi, Makoto Asai, Yasuo Arai

HUPD-9003, Jan. 16, 1990

On-chip Filtering of Low P_t Track with Straw-Tube Chamber

Takashi Ohsugi
Department of physics, Hiroshima University.
Makoto Asai
Hiroshima Institute of Technology
Yasuo Arai
National Laboratory for High Energy Physics, KEK

Abstract

On-chip filtering of low P_t background track mainly from minimum-bias events is proposed. Hardware recognition of high P_t track is essential for the second level lepton trigger. Low P_t track filtering without track reconstruction is also essential for quick search of interesting high P_t event in the off-line analysis, otherwise one may need unrealistic amount of CPU power to analyze the data at the SSC experiment.

Introduction

We are going to pursue new physics which will be emerge as high P_t phenomena at the SSC experiments. Immediate finding of high P_t track is essential for high P_t lepton trigger which is expected to be the most effective and important for new physics at SSC experiments. The straw-tube chamber are proposed for an important part of the central tracking system of general purpose 4π detector because of its excellent pattern recognition capability. Here we studied the fast track finding method of high P_t track with superlayer- structured straw chamber for trigger purpose as well as noise and low momentum background filtering. This function can be easy implemented on the time memory cell(TMC)[1] which is being developed for a high rate drift chamber at KEK.

Superlayer structure of straw-tube chamber has been proposed for the central tracker of general purpose magnetic detector[2]. Superlayer structure has an advantage for recognition of track element in a heavy background. This scheme also well match to the TMC readout. Here we propose a TMC readout with on chip filtering and show how well the filtering works by using simulation.

Straw-tube tracking system

We assumed that three superlayers of straw-tube chamber are placed at the radial distance of r=126 cm, 141cm and 156cm. Each superlayer consists of the half-cell staggered eight layers of straw-tube chamber. Straw diameter is 6mm. For simplicity, the straw-tube chamber is assumed to be one unit of long tube covering the pseudo-rapidity range listed in Table 1. Superlayer structure of straw-tube chamber is the same as the LSD design [2] as shown in Fig.1. Uniform solenoidal field of 2 Tesla is assumed inside the tracking volume in this study. Silicon strip chambers are implemented inside the straw-tube chamber to help imagine events as realistic as possible.

Filtering Scheme

We expect to observe an interesting event which is overlapped with few minimum-bias background under the condition of the standard SSC luminosity of 10^{33} cm^{-2} s^{-1}. Transverse momentum (P_t) of the particles produced by the minimum bias events peeks around 400 MeV/c and most of the secondary particles have transverse momentum less than 1 GeV/c as shown in Fig.2. Curling tracks will give very severe background to the tracking system. However, their transverse momentum must be less than 600 MeV for 2 Tesla field and 2 m radius volume. Therefore, if we set threshold of P_t filtering around one GeV which is still safety enough for detecting high P_t new Physics, we can discriminate most of the background tracks from minimum biased events.

Let's look at structure of the straw-tube chamber proposed here as shown in Fig. 1. Four cells aligns on the straight line from the interaction point, which means that these four cells can detect high momentum straight track or reject low momentum slant track. We examined momentum acceptance of these aligned four cells under the track recognizing condition of 3 out of 4 coincidence by changing chamber efficiency. Resulting acceptance for outer most superlayer is presented in Fig.2. P_t cut looks excellent for discriminating tracks from the minimum-bias background. This fact suggests that hit or no-hit information of straw-tube is very useful for trigger and background filtering. If we take a coincidence of signals from three superlayers in the unit of $\Delta\Phi=\pm0.01$ radian (~three consecutive columns) as shown in Fig.3, threshold momentum goes up to several GeV/c which is still low enough to detect high Pt Physics. This filtering scheme can be easily installed in the TMC[1] chip as shown in Fig.4.

Results of Performance simulation

In order to demonstrate the performance of this filtering scheme, we generate minimum-bias events by PYTHIA event- generator and pass them through GEANT 3 to make realistic detector signals. Then we superimpose 5 events and submit to the filtering scheme mentioned above. Table 1 shows the number of hits in each superlayer, surviving hit-cells after imposing 3 out of 4 filtering and signals left after taking further three hold superlayer coincidence. The filtering of 3 out of 4 coincidence in each superlayer can reduce signal outputs down to about an order of magnitude. Further requirement of three superlayer coincidence can reduce one more order of magnitude.

Table 1.
Number of hit-cells for 5 minimum-bias-event overlapped
(averaged over 100 samples)

radial distance (cm)	No. of hit-cells	3/4 coinci. on each superlayer	3 hold coinci. of superlayers
126	1110	130	6.5
141	1093	95.7	6.7
156	921	64.2	6.0

The event of Higgs particle decaying into 4 muons superimposed by 5 minimum-bias events is displayed in Fig. 5-a. In Fig. 5-b signals expected from this model central tracking detector are depicted. After imposing the filtering of 3 out of 4 coincidence at each superlayer of straw-tube chamber, survived hit-cells are displayed in Fig. 5-c. One can clearly see that most of the low- P_t and curling track's hit-points are wiped out. Furthermore taking coincidence of three superlayer picks up four muons decayed from Higgs particles and only two additional tracks as shown in Fig. 5-d. In this stage, associations of track and EM calorimeter informations will be easy examined by appropriate hardware processor for second level electron trigger. Fig.6-a, 6-b, 6-c and 6-d shows the event of Higgs decaying into four

jets overlapped with five minimum biased background. Other conditions are the same as Fig.5.

This filtering scheme is also very effective to save analysis time and CPU resource, because we can reject 99 % of background tracks without performing track reconstruction at off-line analysis.

References

1) Y. Arai and T. Ohsugi, Proceedings of 1986 Snowmass Summer Study, p455.
   Y. Arai and T. Ohsugi, KEK preprint 88-87, Nov. 1988.
   Y. Arai, KEK preprint 88-130
2) R.DeSalvo, Proceedings of 1986 Snowmass Summer Study, p391.
   G.G.Hanson, S.Mori, L.G.Pondrom and H.H.Williams, Proceedings of the Workshop on Experiments, Detectors, and Experimental Areas for the Supercollider, July7-17, 1987 Berkeley, California, p340.

Figure Captions

Fig. 1 Superlayer structure of straw-tube chamber proposed by LSD group.

Fig. 2 Acceptance of 4 cells aligned on the straight line from the interaction point is shown together with transverse momentum distribution of secondary particles in minimum biased events.

Fig. 3 Transverse momentum acceptance of the filter imposing three hold coincidence of three superlayers.

Fig. 4 On-chip filtering planned on a TMC chip for the signals from the the straw-tube chamber having superlayer structure.

Fig. 5-a The event of Higgs particles decaying into four muons overlapped by five minimum-bias events.

5-b Signals taken from the same event as 5-a by the model detector.

5-c Surviving signals through 3 out of 4 filtering in each superlayer.

5-d Surviving signals after 3 hold coincidence of three superlayers.

Fig.6-a The event of Higgs particle decaying into four jets overlapped by five minimum-bias events.

6-b Track elements taken by the model detector.

6-c Track element survived through 3 out of 4 filtering on each superlayer.

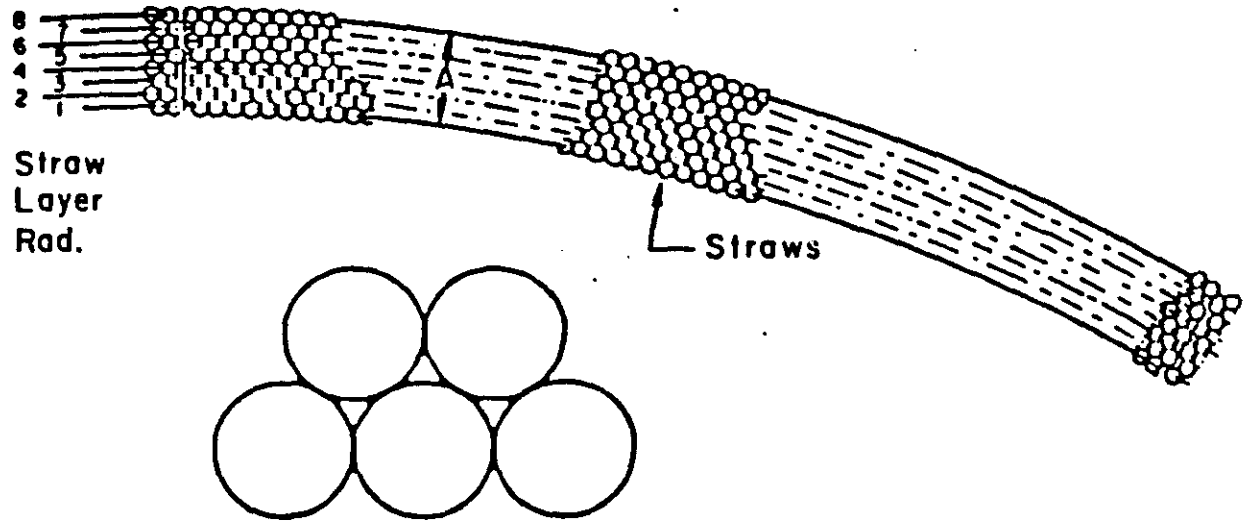

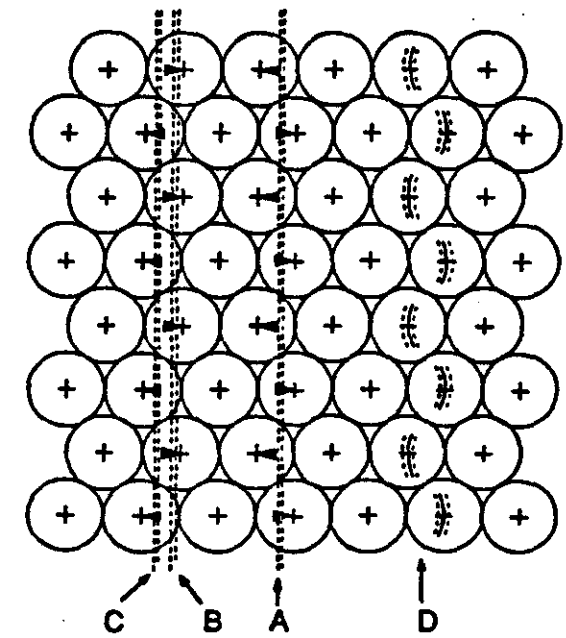

FIG. 1

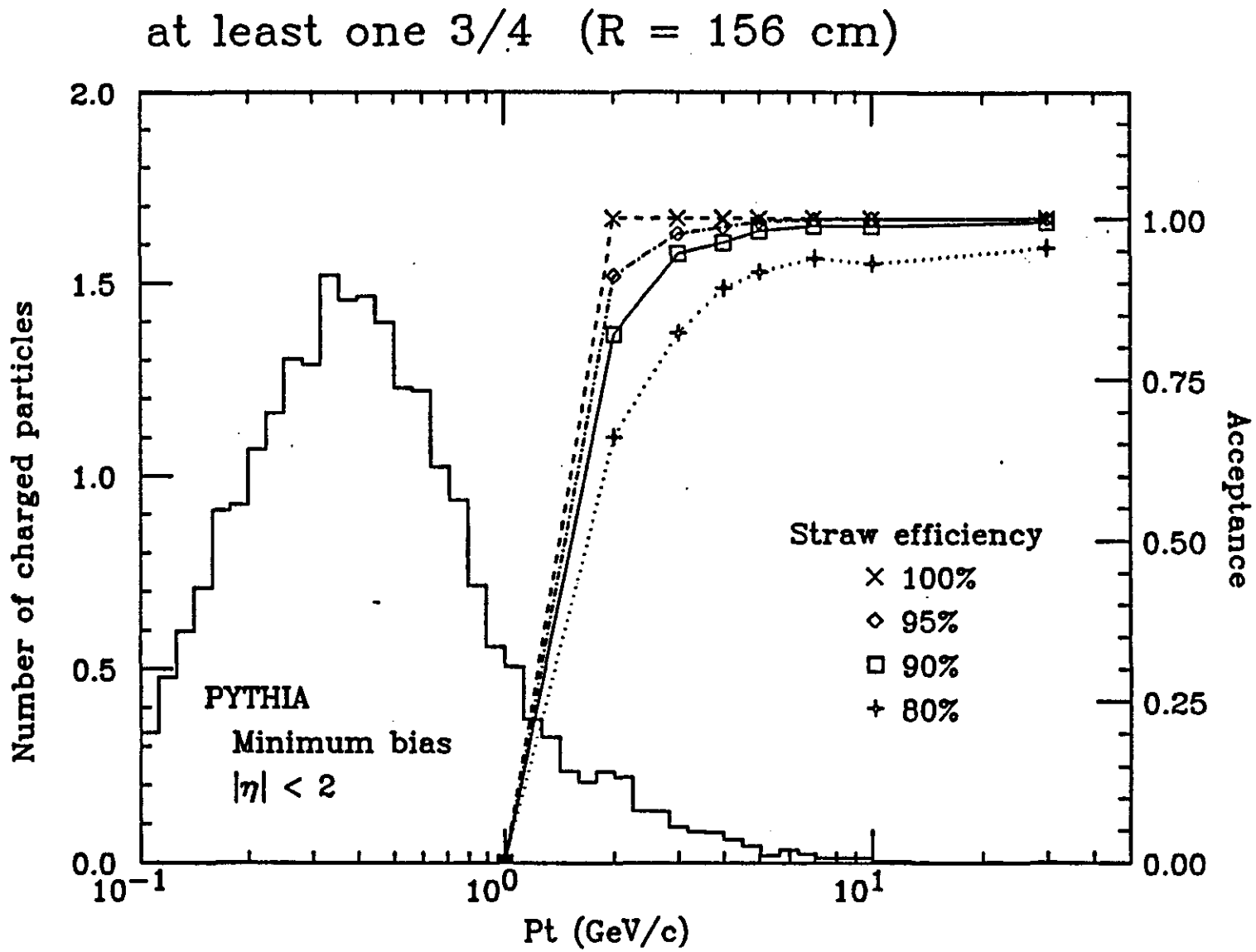
at least one 3/4 (R = 156 cm)
Number of charged particles
Acceptance
Pt (GeV/c)
PYTHIA
Minimum bias
|η| < 2
Straw efficiency
× 100%
◇ 95%
□ 90%
+ 80%
2.0
1.5
1.0
0.5
0.0
1.00
0.75
0.50
0.25
0.00
10^-1
10^0
10^1

FIG. 2

3 S.L. coincidence

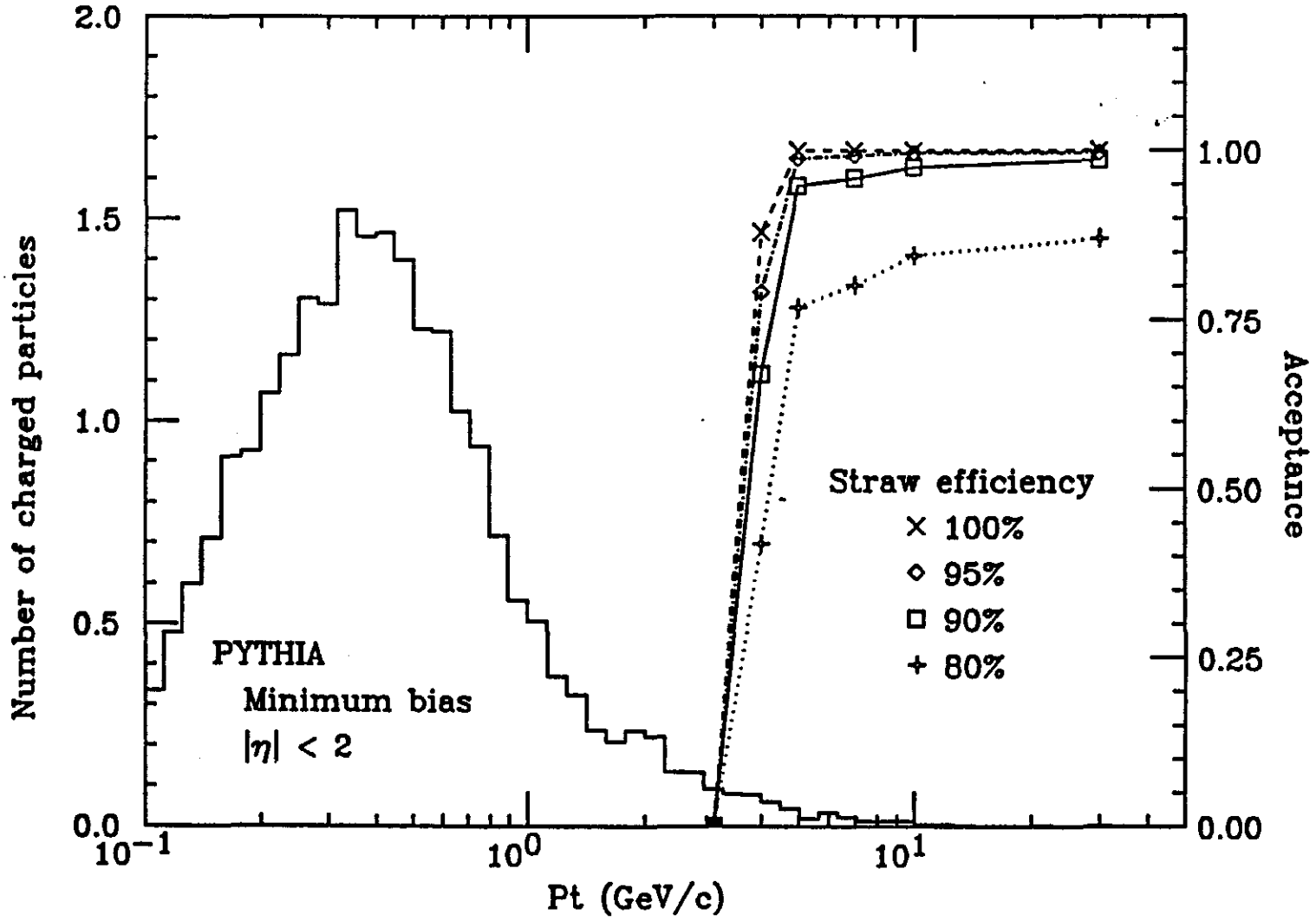

FIG. 3

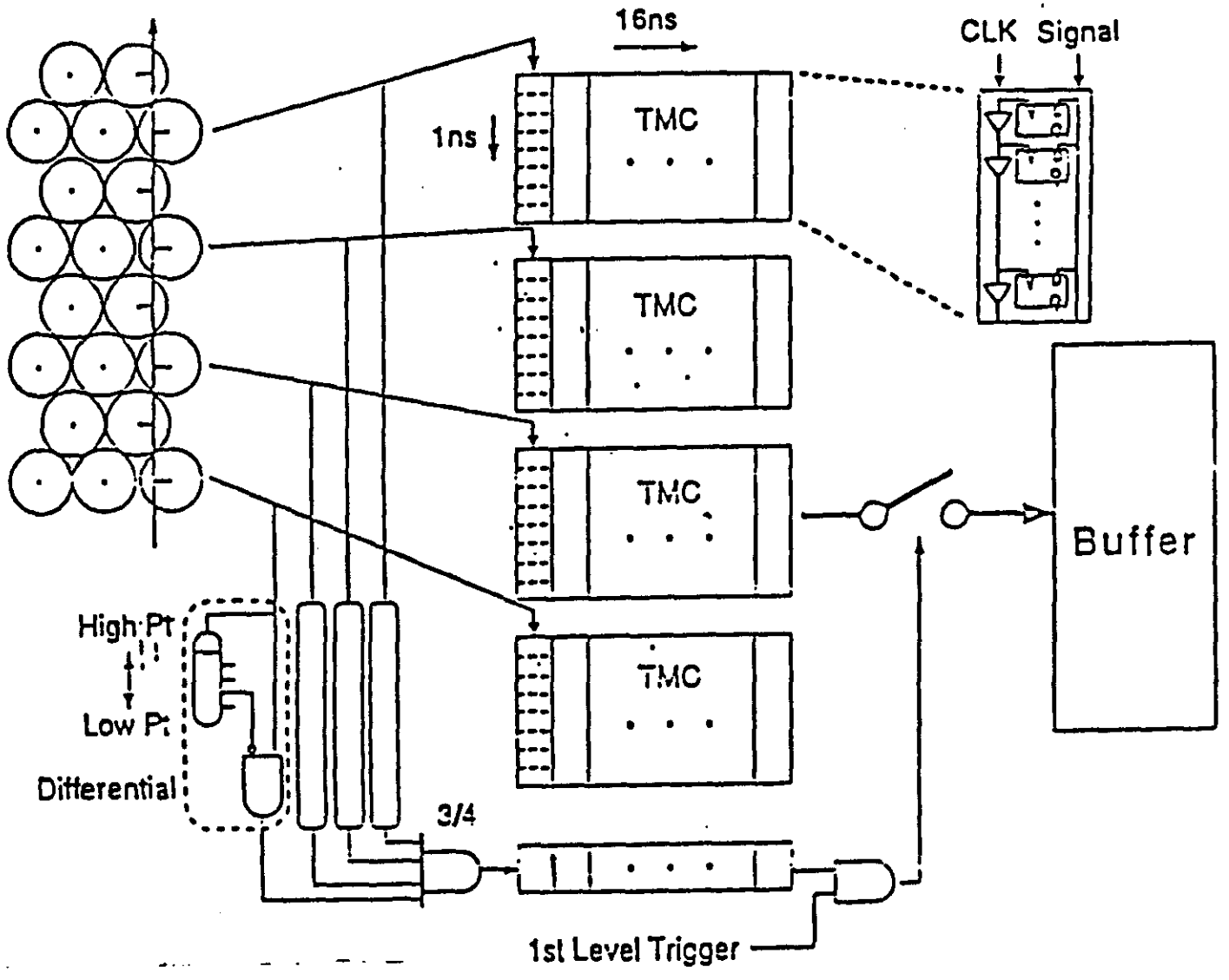

Stiff Track Readout

FIG.

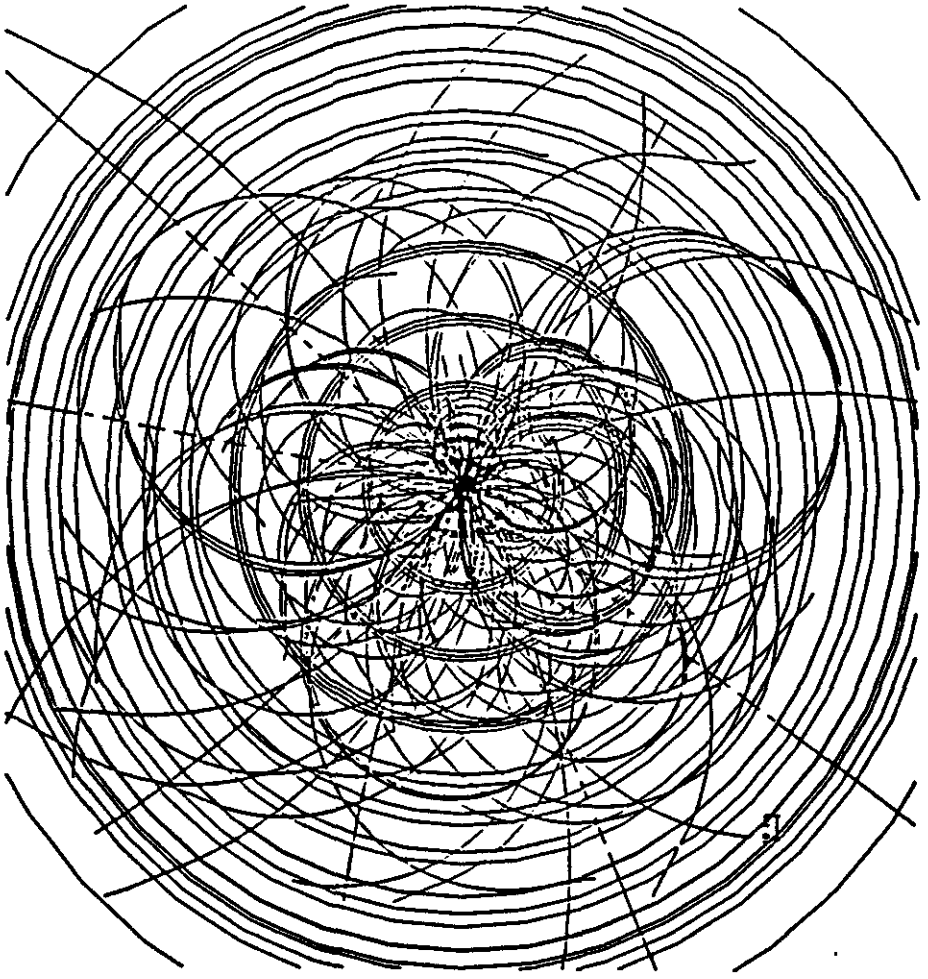

FIG. 5-a
Higgs--4 muons overlapped with five minimum-bias events. The dotted lines indicate the 4 muons.

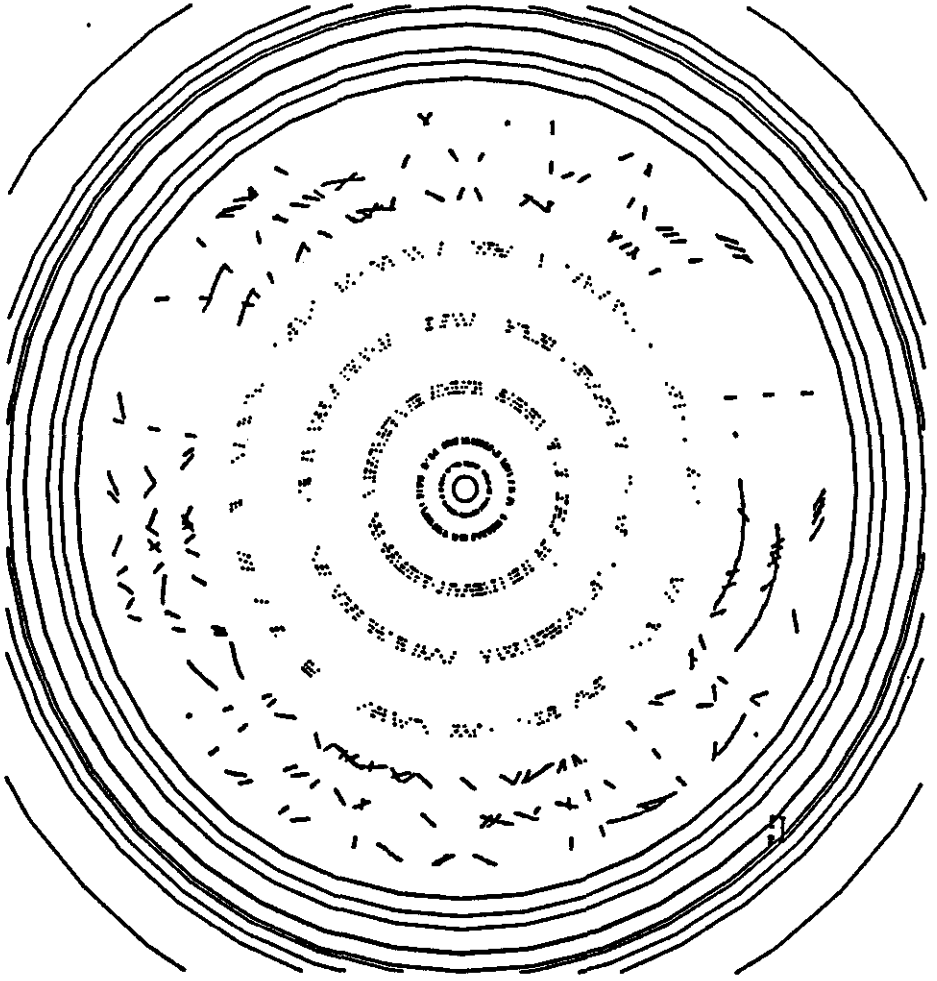

FIG. 5-b

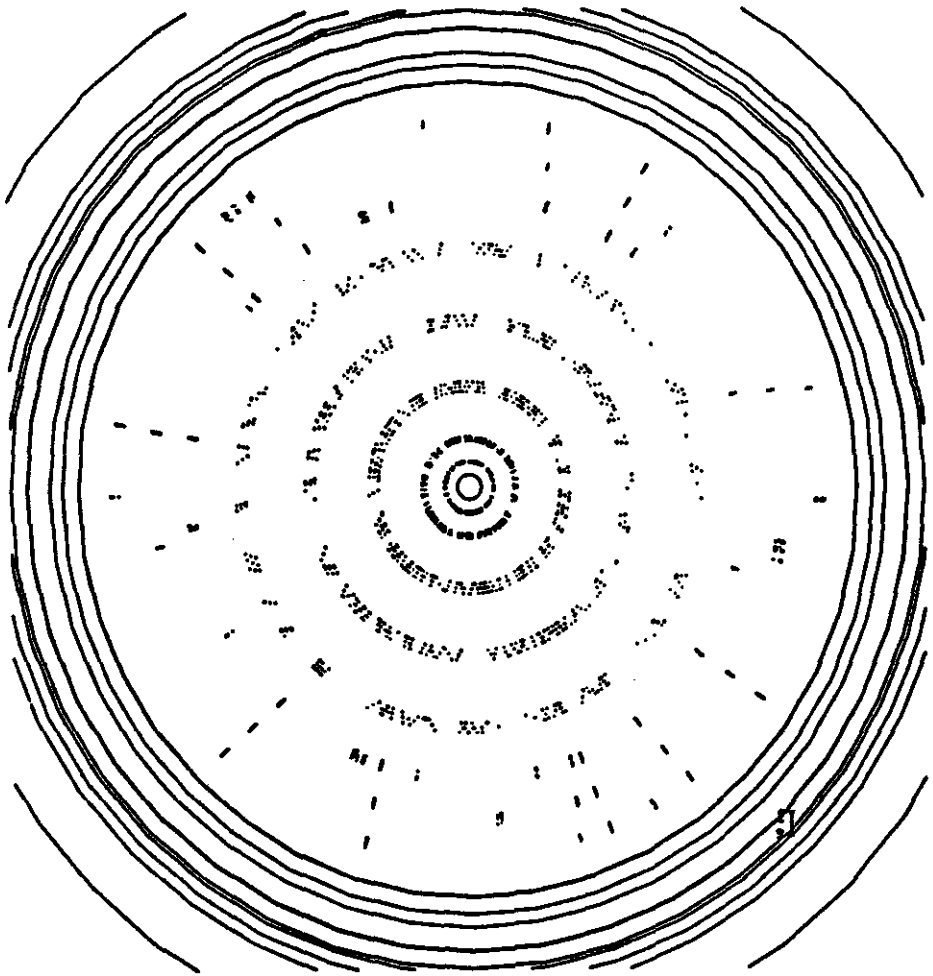

Fig. 5-c

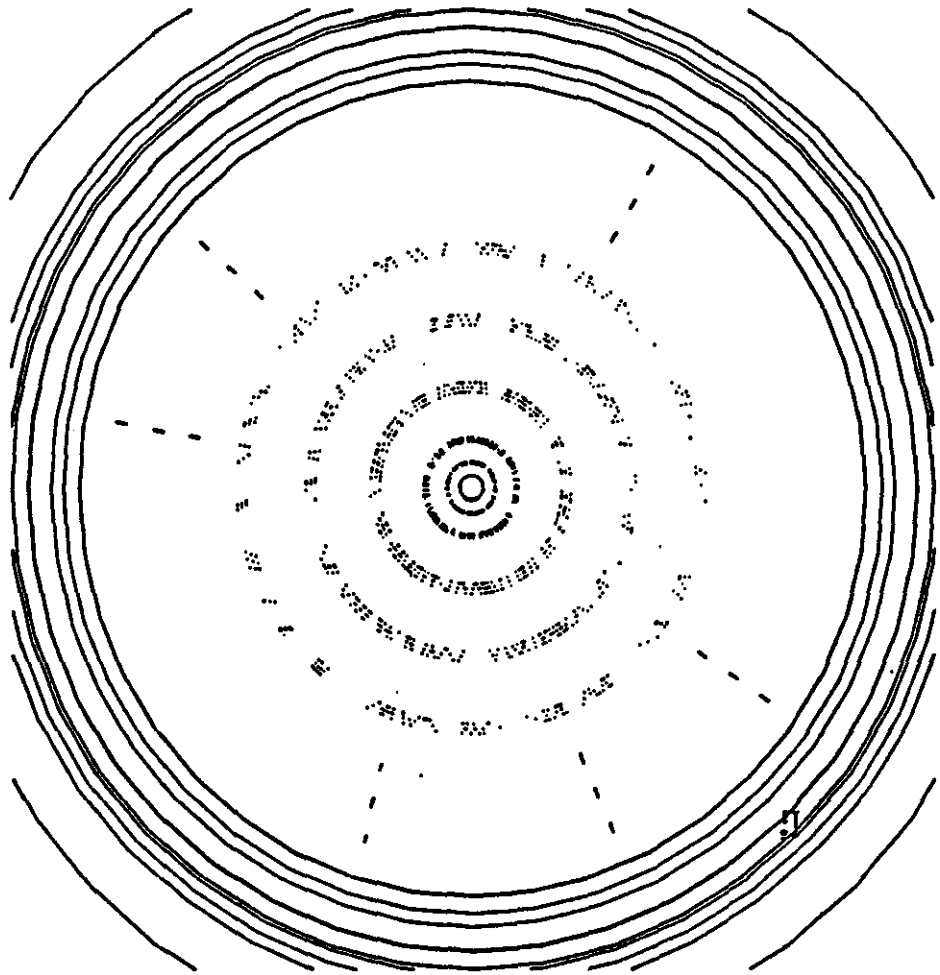

Fig.5-d

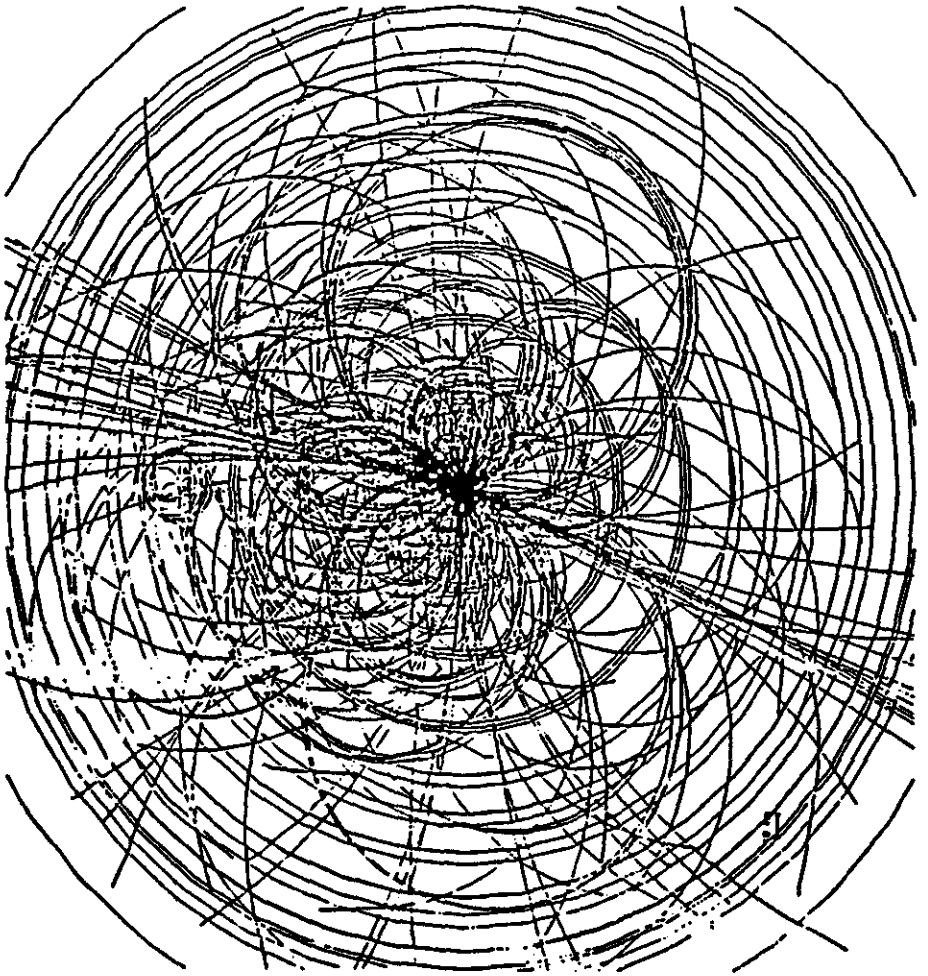

Fig. 6-a

Higgs--4 jets overlapped with five minimum-bias events.

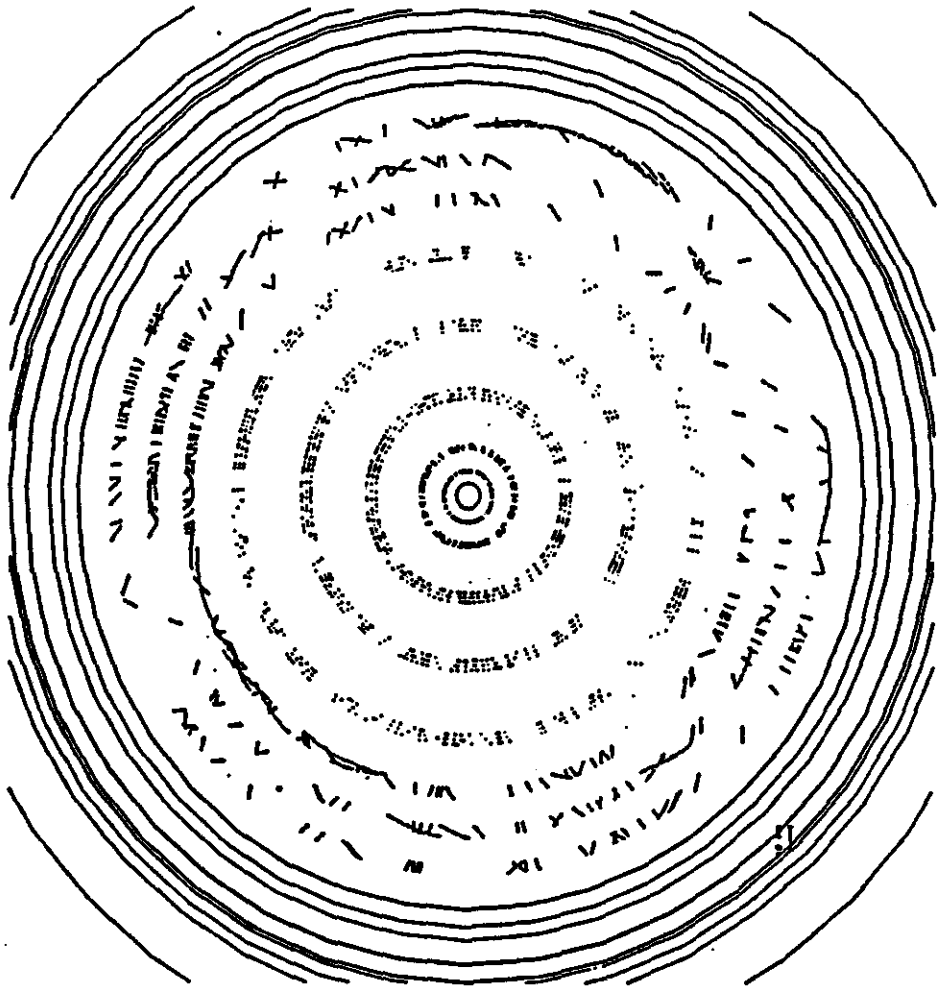

Fig. 6-b

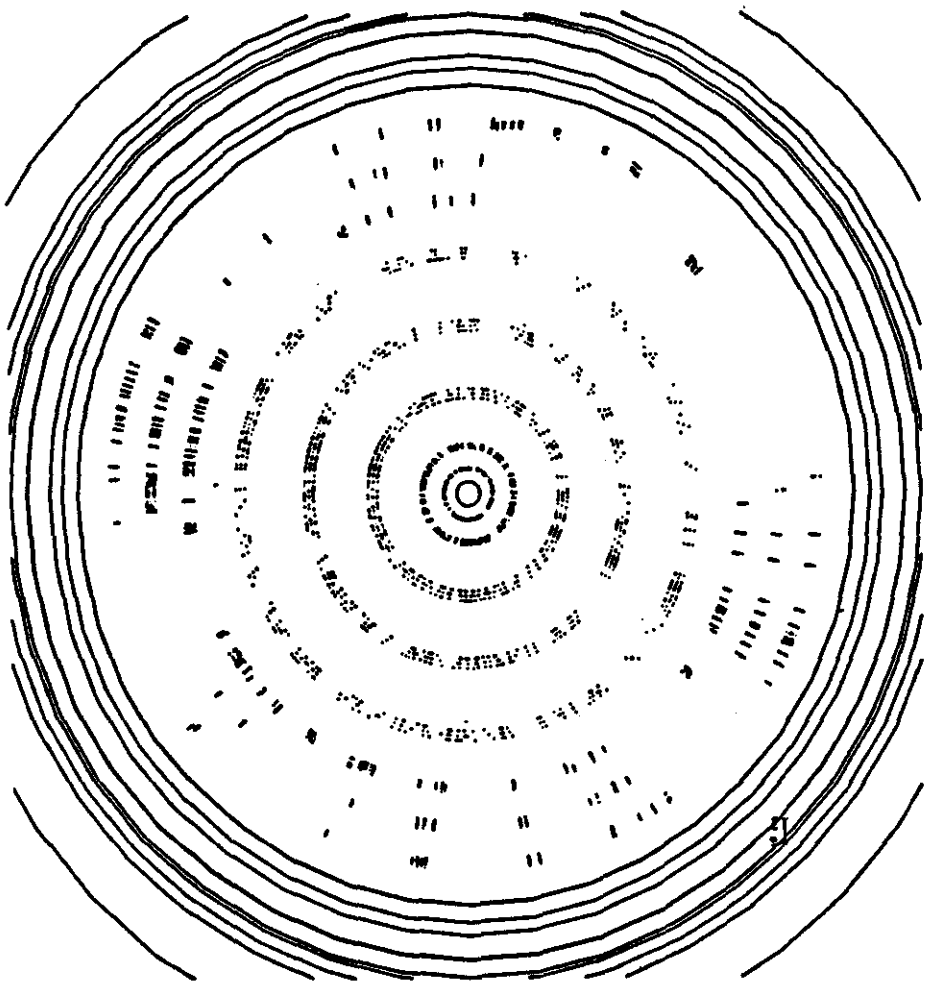

Fig. 6-c

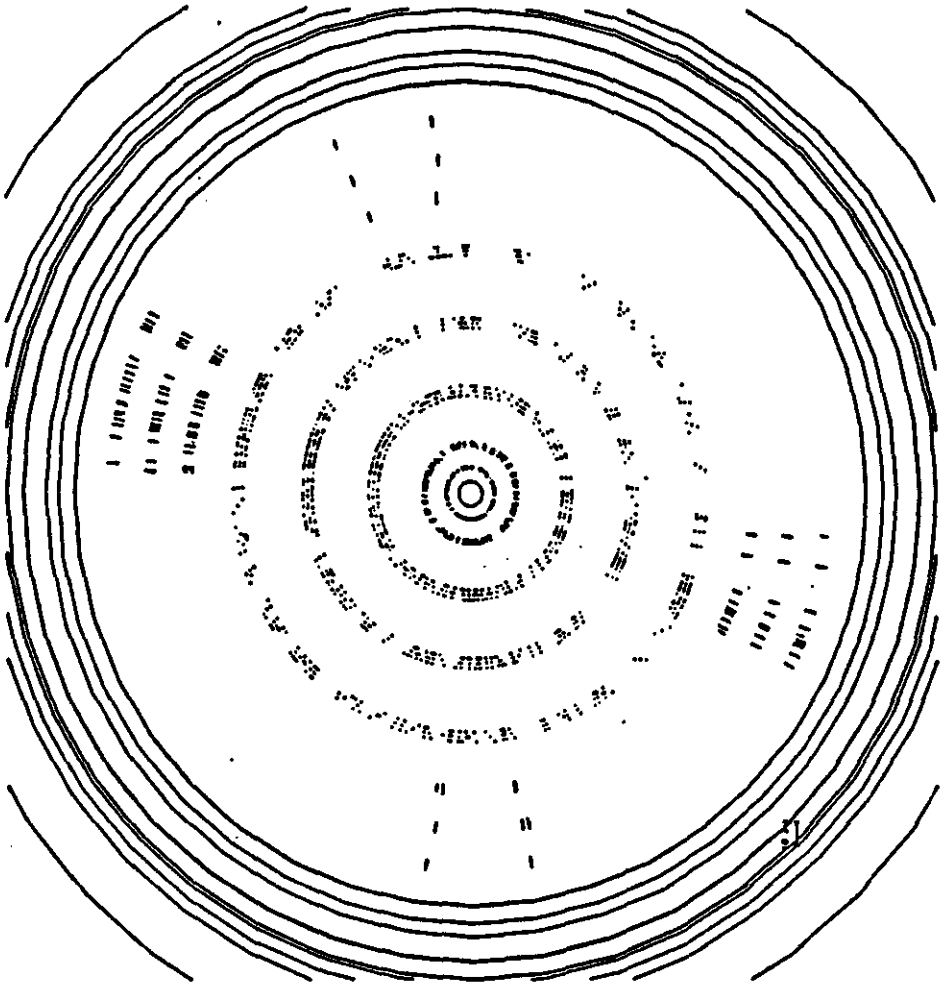

Fig. 6-d

HUPD-9002
Jan. 16, 1990

Central Tracking Devices for the SSC*

Takashi Ohsugi

Department of Physics, Hiroshima University

The central tracking device of the general purpose 4π magnetic detector should satisfy following requirements.

1) Physics requirements

Requirements for the central tracker are closely related to the reasons why we select a magnetic detector. We select magnetic detector to measure the momentum of high P_t lepton or to determine the charge-sign of electrons. Vertex assignment of the each charged particle is also essential for high intensity hadron collider experiments to separate individual event because multiple events in one bucket are expected at the standard SSC luminosity. To maintain the flexibility for new physics and unusual topology, a central tracker is essential. Independent measurement of momentum and energy makes it possible to calculate an invariant mass of interesting object and help to identify electron with E/P ratio. Independent measurement of energy and momentum are mutually compensating and/or important redundancy for correction or calibration.

Momentum resolution required are typically followings;

a) Higgs -- Z Z -- 4 muons (electrons) ($M_H = 400$ GeV/c^2)

$\sigma(P_t)/P_t = 0.3 \times P_t$ (TeV/c)

b) New Gauge Boson $Z -- \mu^+ \mu^- (e^+e^-)$ ($M_Z = 2$ TeV/c^2)

If relative mass resolution of 20% is required for M_Z reconstructed, the necessary momentum resolution is

$\sigma(P_t)/P_t = 0.15 \times P_t$ (TeV/c)

Pseudo-rapidity coverage of fine resolution central tracker should be ~1.7 by requirement of more than 80% detection efficiency for Higgs--$\mu+\mu-\mu+\mu-$[1].

Fast track-finding capability for high P_t isolated track is also essential to trigger with high P_t electron candidates combined with EM calorimeter information.

2) Survivability

a) Hit-rate

The central tracking device should survive at the standard SSC experimental luminosity for 10 years. High rate capability as well as radiation hardness becomes the most severe requirements for the SSC central tracking device. For example, hit-rate of a 5mm Φ straw covering $|\eta| < 1.5$ has been calculated by M.Asai[2]. This simulation has been performed with GEANT by taking into account of all secondary interactions in the detector materials such as gamma conversions and multiple scattering etc. The field strength is assumed to be 2 Tesla uniform solenoidal field. The calculated hit-rates are presented in Fig.1. Reasonable hit-rate of straw-tube chamber seems to be less than 1 MHz by considering many problems such as a chamber life time, signal pile up and hence degradation of chamber efficiency etc. The minimum gas gain required for reasonable time resolution i.e. reasonable position resolution has been studied by H.Iwasaki[3]. More than 10^5 gas gain is required for 150 μm position measurement resolution with 5m straw tube. High capacitance of long straw causes poor rise time of signal. With optimized time constant (~15 ns) of pulse shaping for the time resolution and signal pile-up problems, it is necessary about 100 ns to be ready for the next signal. Both studies suggest that we have to install a short straw-tube chamber outside 1m distance from beam line.

Hit-rate of the silicon strip detector is expected to be small and no problem because of its small size. For high speed readout, intrinsic large capacitance of silicon detector may degrades signal to noise ratio, which will be solved with optimization of strip size and position resolution.

b) Radiation damage

Radiation damages becomes serious for the detector placed close to the beam line. Estimated radiation levels are reported in the CDG report edited by D.Groom[4]. In this report, charged particle flux calculated with total cross section is given by

$$dN_{charged}/da = (1.2 \times 10^8\ s^{-1})/r_t^2,$$

where da is a normal area element and r_t is a perpendicular distance from beam line. In a light material energy loss, dE/dx is nearly equal to 1.8 MeV $g^{-1}cm^2$, so 1 Gy corresponds to 3×10^9 particles /cm^2. For example, at $r_t = 10$ cm^2 integrated flux of charged particles amounts to ~ 10^{13} particles /cm^2/year (one year=10^7 s). Most of the neutrons are albedo neutron from calorimeter whose energy is an order of MeV, so that neutron flux is considered to be

uniform in the cavity of calorimeter. An annual fluence of 2.4×10^{12} neutrons/cm^2 is expected inside a spherical cavity with 2 m radius. A general purpose 4 π detector has the calorimeter whose cavity has at least twice as large as the volume of the 2 m radius sphere. Since the neutron flux must be inversely proportional to the cavity volume, the value of 2×10^{12} neutrons/cm^2 used for the radiation damage estimation might be too large. Photon fluence is estimated to be 10^{12} /(cm^2 year) with E>0.1 MeV for the r=2m cavity.

Radiation damage of wire chamber has been studied and summarized in the CDG report[5]. A safety limit of integrated charge might set at 0.1 C/cm for a design of practical chamber and they concluded that aging of wire chamber was not problem at distance from the beam line larger than 50 cm.

For the radiation damage of silicon detector, we have performed experiments by charged particles[6] and neutrons[7]. Radiation damage affects leakage(dark) current, pulse height and operational voltage. The leakage current increases proportional to radiation dose and it presents an index of radiation damage of silicon detector. A proportionality constant of the leakage current is defined by

$$\Delta I_{leak} = \alpha_{c,n} \times \Phi_{c,n},$$

where ΔI_{leak} is increase of leakage current, α_c or α_n are leakage current constants and Φ_c or Φ_n are fluences of charged particles and neutrons respectively. The constant obtained from experiments are

$$\alpha_c = 3 \times 10^{-17} \text{ A/cm},$$
$$\alpha_n = 7 \times 10^{-17} \text{ A/cm},$$

for one particle passing through unit depletion volume. These values are consistent with other experiments. By multiplying an annual fluence for a 25μ x 20 cm x 300μ strip, leakage current increase of 0.55mA per year is expected at the distance of 10 cm by folding both charged particles and neutrons effects. Since this value is not negligiblly small for ten years operation, replaceable structure is recommended within r_t<20 cm. We may cope with saturation of preamplifier with the leakage current by introducing capacitive coupling readout scheme.

Pulse degradation has been observed with 10% for 2.5×10^{13} neutrons/cm^2 which corresponds to ten years operation[7]. Neutron damage seems not to be serious, but charged particles may causes significant pulse degradation because of its an order of magnitude higher flux at 10 cm from beam line.

Conceptual design of hybrid central tracking system

A cylinder of 170 cm radius and 8 m long is set as a tracking volume for this design study. The reasons why we select this size are to compromise the calorimeter cost and achievable tracking performance. Air-core type solenoid is chosen to attain a excellent hermeticity of calorimeter in this detector design. Obviously disadvantage of the air core type solenoid is claimed from non-uniform field which gives some difficulties for the tracking and momentum measurement. We can cope with this disadvantage by using compact silicon detector at uniform field region. Track reconstruction in the non-uniform field is demonstrated in the AMY experiment at TRISTAN and seems not to be problem[8].

Design concept of this hybrid tracking detector is a separated function tracker. The momentum resolution is mainly attained by the silicon detector. Pattern recognition, tracking and trigger requirements are achieved by straw-tube chamber which is placed in a region more than 1 m from the beam line.

Straw-tube chamber

In the barrel part, four superlayers of radial straw chamber are planed outside the radius of 1m cylinder as shown in Fig.2. Those parameters are shown in Table 1. Barrel part covers $|\eta|<1.5$. Each superlayer consists of 8 layers of ~7 mm straw-tube. In order to cope with high rate and high capacitance problem, we segment straw-tube chamber three parts, resulting in 1.6m~2.2m long straw and hence 20 pF readout capacitance. The straw-tube of this size can be operated with 10^5 gas gain and expected reasonable performance as shown in Table 2. We expect that position resolution of each straw-tube is better than 200μm. We can probably handle setting error of straw-tube within 50μm. Then we expect overall resolution close to 200μm. The superlayer structure of straw chamber has a excellent capability of immediate recognition of stiff track element[9] in rather heavy background. We emphasize an importance on this feature in the viewpoint of high Pt lepton trigger and patter recognition.

We plan to measure a Z coordinate as a propagation time difference between both ends. Time resolution of 0.5 ns corresponds to 5 cm resolution of Z coordinate. Although 5 cm resolution sounds very poor, one by one

association of three dimensional coordinate is very important to reconstruct a track in three dimensional space in the high multiplicity environment.

Readout electronics is designed by using the time memory cell (TMC) which is being developed at KEK[10]. The TMC can digitize the time directly and have a pipe-lined digital memory by itself. Total readout channels are 230 k including both end readout for the barrel part. Power consumption of readout electronics is estimated to be 30 mW per channel including all electronics installed at the detector (preamplifier, shaper, discriminator, TMC and digital processing electronics). We clearly need some cooling system for the readout electronics.

Endcap is composed of four disk shape detector for both side. Each disk-shape detector consists of u, v and w plains of straw-tube chamber. The v and w planes rotate clockwise and counterclockwise with 60 degrees from the u plane axis as depicted in Fig. 3. Each u,v and w plane is composed of 8 layers of straw-tube. It is segmented that tube length becomes less than 2 m. Signal is readout from outer side in order to put electronics away from beam line. Total readout channels of forward straw chamber amounts to 145 k channels for both end. Parameters for endcap straw-tube are listed in Table 3. Material thickness is estimated to be ~4% radiation length (X_0) at 90 degrees and increases gradually to ~8 % approaching to $|\eta|=1.5$. At the endcap part, amount of material is three times thicker than that of barrel part, which is ~12.5 % X_0. The η dependence of material thickness for straw chamber is shown in Fig. 7-a.

Silicon Strip Detector

a) Detector

Silicon strip detector is selected as a inner tracking device because of its precise position measurement and high rate capabilities. The momentum resolution of this tracking system is mainly relied on silicon strip detectors. Since magnetic field strength and tracking length is limited by engineering and cost limitations, precise position measurement is required to determine the momentum of high energy particles. High ability to separate two tracks is also significant advantage to identify the lepton track in a hadron jet.

For the barrel part, eight sets of two layers unit of cylindrical silicon detectors are placed at the radius of r=10cm to r=82 cm as shown in Fig 2. The strip spacing and strip length for each layers are listed together with expected spatial resolution in Table 4. For this size, capacitance of each strip

will be less than 20 pF. Why we choose linearly increasing strip width is to reduce the readout channels. This is the most economy way to measure particle momentum when the vertex position is in a region localized enough[12]. This scheme matches well with rather poor resolution of outer straw-tube chamber. We calculated momentum resolution both structures of a equal spacing layer and a superlayer structure. The equal radial spacing model has slightly better resolution but difference is very small so that we choose a superlayer structure which gives a better pattern recognition capability and favorable conditions for a fabrication and cooling.

We would like to employ a double sided strip detector to readout two dimensional information with detectors as thin as possible. The double sided strip detector was recently studied by Holl et al.[13]. Now mass production techniques are being studied by the collaboration of Nagoya University and Hamamatsu Photonics.

In order to reduce readout channels, we select the capacitive charge division readout. For 25μ strip pitch detector, every three strip is connected to readout electronics, so that readout strip pitch becomes 75μ. Capacitance of each strip is estimated to be ~5pF by assuming 300μ depletion depth. A signal to noise ratio of 15 can be attain for this readout scheme[14]. For 50μ and 100μ pitch detector, every other second strip is connected to readout electronics. We need more study of a backside readout scheme of the double sided detector.

Forward detector will cover the pseudo-rapidity range from 1.5 to 2.5 as shown in Fig.2. The fan-shape strip is occupied a the same azimuthal angle of 0.25×10^{-3} radian which corresponds to 25μ strip pitch at r=10 cm. The fan-shape strips are radially segmented to reduce the readout capacitance reasonably. The geometrical parameters for the endcap silicon detector are tabulated in Table 5. Hit-rate per strip is calculated to be an order of 50 kHz taking into account of secondary interactions and curling track. The charge division readout is applied to this part. Every other strips are connected to the readout electronics except for the largest strip, the most outer part of the largest disk. For this strip, readout electronics will be connected one by one strip because of high capacitance. The number of readout channels are counted up to 240×10^3 for the momentum measurement side. A slant strip method are used to measure a radial position with backside strip. The stereo angle of 3-5 degree is adapted because the millimeter precision is enough for pattern recognition on the r-z plain. The number of readout channel is the same order as the front side.

b) Readout Electronics and Power Consumption

Readout electronics may be key point to realize a large scaled silicon strip detector for the SSC experiments. Packing density of the front-end analogue electronics chain has to be compatible to the strip pitch. Radiation hardness should be as good as the silicon detector itself. We are going to develop a bipolar preamplifier+shaper+comparator LSI for digital readout at NTT[11]. The super self-aligned transistor (small size and hence extremely high speed) is applied to make a high speed but low power front-end electronics. High current density of SST transistor gives radiation hardness. We have examined radiation hardness of SST transistor by neutrons[15] and gamma-ray[16]. Results are very promising that it can survive with 10^{13} neutrons per cm^2 and with the gamma rays of 10^6 rad.

We will select digital readout scheme which can process data on the detector and reduce its size to eliminate enormous amount of cable. Signal induced on a strip detector is amplified, shaped and discriminated in a bipolar LSI. Since only on-off information of each strip is obtained, the position resolution is given by the strip pitch. This readout scheme must be the most resistant against noise. Then digital processing LSI processes those data and suppresses zeros. Since occupancy of silicon detector is very small, data size can be reduced to more than one thousandth. Detail readout scheme has not yet designed.

Power consumption of this LSI is calculated to be 7 mW per channel including preamplifier, shaper and discriminator. Digital processing unit are being developed at Santa Cruz by rad-hard CMOS process. Power consumption combined with analogue part and digital part is expected to be 8 mW per channel which means 8 kw for million channels. Power-feed and cooling for the readout electronics sounds a key issue of the silicon strip detector.

c) Integration of silicon detector

Integration of silicon detectors and readout electronics is another important issue. Since we are going to use the double sided detector, micro connection technique has to be utilized in both plane of the micro-strip detector to readout signals. The combination of a tape-automated bonding(TAB) and a wire bonding may be proper technique for integration of the strip detector and readout microelectronics. Fig.4 shows a sketch of one detector unit proposed. Connections between detectors are made with TAB at the back-plane and with

wire bonding at up-side respectively. Schematic picture of a dead-angle-less integration of unit detector is depicted in Fig.5.

d) Cost Estimation of silicon detector

Most economical way of silicon detector production is achieved by following with industrial standard. A 300μ thick and 4 inch diameter wafer of high-resistive, detector grade silicon is available with reasonable price. If we think about fabrication of many pieces of silicon detector precisely, the largest piece taken from standard 4 inch wafer is obviously prefer for fabrication. Thus we performed this design study with 6.4 x 6.4 cm^2 (sensitive area) piece which is the largest size taken from the 4 inch wafer. Number of pieces needed to cover the detector designed here are listed in Table.4 and 5. Total number of pieces we need are about 30 k for barrel part. and 3.6 k for forward part. We hope that the price of double sided strip detector is to be ~$1000 per one piece, if we establish a mass production technique. Then the total cost of the silicon detector amounts to $34 million.

Momentum resolution and Material Thickness

The rapidity dependence of transverse momentum resolution at 1 Tev/c is depicted in Fig.6. In this calculation, we assume uniform 2 Tesla field and gaussian shape error of position resolution listed in the parameter Table 4 and 5. If we take into account of field decline at the edge region of ACS magnet, momentum resolution at η=1.5 degrade ~5 %[8]. The line a) , b), and c) indicate momentum resolution expected from following configurations;

a) momentum resolution expected by using all silicon layers and straws.
b) eliminating four layers of silicon strip detectors placed at r=70, 72, 80 and 82 from original design for barrel part, and for the endcap part eliminating central plane in each consecutive three planes.
c) without six layers of silicon strip detectors placed at r=10, 12, 50, 52, 80 and 82 cm from original design for barrel, and for endcap the same configuration as b).

The configuration b) is aimed for reducing significant amount of readout channels, saving 1.1 million channels. Weak point of this configuration may be pattern recognition capability, because of large gap between silicon and straw chamber. The configuration c) is the proposal for reducing readout channels and also reducing radiation damage problem. In this calculation, we neglect setting errors of all detectors, and the effect from missing points

due to detector inefficiency and/or noise and background overlapped. We have to develop pattern recognition program together with momentum reconstruction to study which is the best configuration.

Material thickness for above three configuration are calculated. In order to evaluate realistic material thickness of the silicon tracker part, we assume that an average thickness including all materials for structure and cooling is twice of silicon detector thickness. The pseudo-rapidity dependence of silicon detector thickness is presented in Fig. 7-b. It looks quite thick. We may suffer from heavy gamma conversion problem. We have to compromise the momentum resolution and the material thickness for realistic tracker design.

Acknowledgements

We acknowledge valuable discussions with T. Kondo and S. Sugimoto.

References

* Contributed paper for the Workshop on Haron Collider Physics, Tsukuba Univ., Sep. 16-17, 1989. This report is based on the results from a group study of following people; K.Amako, M.Asai, Y.Arai, H.Iwasaki, Y.Takaiwa and T.Ohsugi

1) Y.Asano, Muon Detector 1, in this proceedings.

2) M.Asai, Hit rate of the Straw Chamber, in this proceedings

3) H.Iwasaki, A Study on Time Resolution for a Straw Chamber, KEK Preprint 89-158, Nov. 1989

4) D.Groom, Radiation levels in the SSC Interaction Regions, SSC -SR-1033

5) G.Gilchriese, Radiation Effects At The SSC, SSC-SR-1035

6) T.Ohsugi et al., Nucl. Instr. and Methods, A265(1988)105
M.Nakamura et al., Nucl. Instr. and Methods, A270(1988)42

7) M.Hasegawa et al., Nucl. Instr. and Methods, A277(1989)395
T.Arima et al., Japanese Journal of Applied Physics, 28(1989)1957

8) T.Takaiwa, private communication.

9) M.Asai, T.Ohsugi and Y.Arai, On-Chip Filtering of Low Pt Track with Straw-Tube Chamber, in this proceedings

10) Y.Arai and T. Ohsugi, 1986 Snowmass Summer Study, p455.
IEEE NS Symposium, October 21-23, 1987.
Y.Arai and T.Baba, IEEE Cat. No88 TH 0227-9
Y.Arai and T.Ohsugi, KEK Preprint 88-78, November 1988, H/D

11) H.Ikeda, KEK preprint 89-7, April 1989, H/D

12) A. Seiden, private communication. F.Abe, private communication, he is now proposing new fast-tracking algorithm.

13) P.Holl et al., IEEE Trans. Nucl. Sci. 36(1989)251.

14) M.Nakamura, private communication.
T.Ohsugi and Y.Tajima, Position Resolution of Micro-Strip Detector and Charge Digitization Resolution, contribution to the workshop on Tracking System for the Superconducting Supercollider, Vancouver, July 1989.

15) H.Ikeda and N.Ujiie, Nucl. Instr. and Methods, A281(1989)508.

16) H.Ikeda and N.Ujiie, Radiation Damage of Bipolar SST Due to gamma-Ray of ^{60}Co, in this proceedings.

Table Captions

Table 1 Parameters of barrel straw-tube chamber.

Table 2 Expected performance of the straw-tube used in our design.

Table 3 Parameters of endcap straw-tube chamber.

Table 4 Parameters of barrel silicon strip detectors.

Table 5 Parameters of endcap silicon strip detectors.

Figure Captions

Fig. 1 Position dependence of Hit-rate (5 mm straw-tube) calculated with PYTHIA+GEANT3 for field strength of 2 Tesla. The secondary interactions such as gamma conversion, nuclear interaction and multiple interaction etc. are all taking into account.

Fig. 2 Layout of central tracking system designed in this study.

Fig. 3 Schematic picture of endcap straw-tube chamber. pseudo-rapidity.

Fig. 4 Schematic view of unit detector composed of silicon strip, readout LSI chips and flexible cables.

Fig. 5 Schematic view of how to integrate unit detector element without crack.

Fig. 6 Transverse momentum resolution at 1 TeV/c as a function of the pseudo-rapidity.

Fig.7-a Pseudo-rapidity dependence of straw-tube chamber thickness.

Fig.7-b Pseudo-rapidity dependence of silicon detector thickness.

Table 1

PARAMETERS OF STRAW-TUBE TRACKING SYSTEM

(BARREL PART)

Superlayer Number	Inner Radius	Straw Length	Straw Diameter	Rapidity Range	Number of Straws	Number of Readout Channels
1	105 cm	180 cm	6.4 mm	0.65-1.5	8256 x 2	33024
2	110 cm	160 cm	7.0 mm	+-0.65	8256	16512
3	120 cm	200 cm	6.4 mm	0.65-1.5	9328 x 2	37312
4	125 cm	180 cm	7.0 mm	+-0.65	9328	18656
5	135 cm	220 cm	7.0 mm	0.65-1.5	9696 x 2	38784
6	140 cm	200 cm	7.25 mm	+-0.65	9696	19392
7	150 cm	210 cm	7.0 mm	0.65-1.4	10768 x 2	43072
8	155 cm	220 cm	7.23 mm	+-0.65	10768	21536

Total number of straws = 114144

Total number of readout channels = 228288

Table 2

Expected Performance of the Straw-tube Used in This Design.

Items	Parameters
Number of superlayers	4
Number of Z segments	3
No. of layers/superlayer	8
Inner radius	105 - 155 cm
Number of straws	1.14×10^5
Rapidity coverage	1.5
Straw diameter	6.4 - 7.3 mm
Straw length	1.6 - 2.2 m
Gas gain	10^5
Current/wire	0.35 μA
Collected charge	0.2 C/cm/10 yers
Hit rate (B=2T)	1 MHz
Detector capacitance	20 pF
ENC	1800 e
Time jitter	0.4 ns
Time walk	1 ns

Table 3 PRAMETERS OF STRAW-TUBE TRACKING SYSTEM

(ENDCAP PART)

superlayer number	z position	radial position	straw length	straw diameter	rapidity range	number of straws	number of readout channels
U1	2.95 m	50-125 cm	75-150 cm	7 mm	1.64-2.45	5140	5140
V1	3.00	50-125	75-150	7	1.64-2.45	5140	5140
W1	3.05	50-125	75-150	7	1.64-2.45	5140	5140
U2	3.25	50-160	105-210	7	1.50-2.50	6394	6394
V2	3.30	50-160	105-210	7	1.50-2.50	6394	6394
W2	3.35	50-160	105-210	7	1.50-2.50	6394	6394
U3	3.55	50-160	105-210	7	1.55-2.55	6394	6394
V3	3.60	50-160	105-210	7	1.55-2.55	6394	6394
W3	3.65	50-160	105-210	7	1.55-2.55	6394	6394
U4	3.85	50-160	105-210	7	1.64-2.65	6394	6394
V4	3.90	50-160	105-210	7	1.64-2.65	6394	6394
W4	3.95	50-160	105-210	7	1.64-2.65	6394	6394

Total number of readout channels = 72966 (for each endcap)

Table 4. PARAMETERS FOR SILICON STRIP TRACKING SYSTEM (BARREL PART)

radial position	strip pitch	resolution	strip length	No.of z segments	readout pitch	capacitance	No.of pieces ϕ	No.of pieces z	No.of pieces	No.of readout channels front	No.of readout channels back
(cm)	(μ)	(μ)	(cm)		(μ)	(pF)				$\times 10^3$	
10	25	7.5	20	3	75	5	12	9	108	30.7	
12	25	7.5	20	3	75	5	12	9	108	30.7	
20	25	7.5	20	5	75	5	22	15	330	93.9	
22	25	7.5	20	5	75	5	22	15	330	93.9	
30	50	15	20	7	100	7	32	21	672	143.4	
32	50	15	20	7	100	7	32	21	672	143.4	
40	50	15	20	9	100	7	42	27	1134	241.9	
42	50	15	20	9	100	7	42	27	1134	241.9	
50	50	15	30	7	100	10	52	35	1820	233.0	
52	50	15	30	7	100	10	52	35	1820	233.0	
60	100	30	30	9	200	20	62	45	2790	178.6	
62	100	30	30	9	200	20	62	45	2790	178.6	
70	100	30	30	11	200	20	72	55	3960	253.4	
72	100	30	30	11	200	20	72	55	3960	253.4	
80	100	30	30	11	200	20	82	55	4510	288.6	
82	100	30	30	11	200	20	82	55	4510	288.6	

Total number of detector pieces = 30648

Total number of readout channels= 2.93×10^6

Table 5. SILICON STRIP TRACKING SYSTEM (ENDCAP)

z Position	Radial Position	Strip Pitch (radian)	Capacitance	Number of Strips	Readout Pitch (radian)	Number of readout channels front plane	back plane
56 cm	10-28 cm	0.25×10^{-3}	4 pF	25120	0.5×10^{-3}	12560	6280
58	10-28	0.25	4	25120	0.5	12560	6280
60	10-28	0.25	4	25120	0.5	12560	6280
80	13-38	0.25	8	25120	0.5	12560	6280
82	13-38	0.25	8	25120	0.5	12560	6280
84	13-38	0.25	8	25120	0.5	12560	6280
110	18-35	0.25	6	25120	0.5	12560	6280
	35-55	0.25	10	25120	0.5	12560	8374
112	18-35	0.25	6	25120	0.5	12560	6280
	35-55	0.25	10	25120	0.5	12560	8374
114	18-35	0.25	6	25120	0.5	12560	6280
	35-55	0.25	10	25120	0.5	12560	8374
140	21-46	0.25	10	25120	0.5	12560	8374
	46-66	0.25	13	25120	0.5	12560	8374
142	21-46	0.25	10	25120	0.5	12560	8374
	46-66	0.25	13	25120	0.5	12560	8374
144	21-46	0.25	10	25120	0.5	12560	8374
	46-66	0.25	13	25120	0.5	12560	8374
170	25-45	0.25	8	25120	0.5	12560	6280
	45-65	0.25	13	25120	0.5	12560	8374
	65-85	0.25	18	25120	0.25	25120	16748
172	25-45	0.25	8	25120	0.5	12560	6280
	45-65	0.25	13	25120	0.5	12560	8374
	65-85	0.25	18	25120	0.25	25120	16748
174	25-45	0.25	8	25120	0.5	12560	6280
	45-65	0.25	13	25120	0.5	12560	8374
	65-85	0.25	18	25120	0.25	25120	16748

Total number of readout channels for each endcap
Front plane= 376800
Back plane = 226092

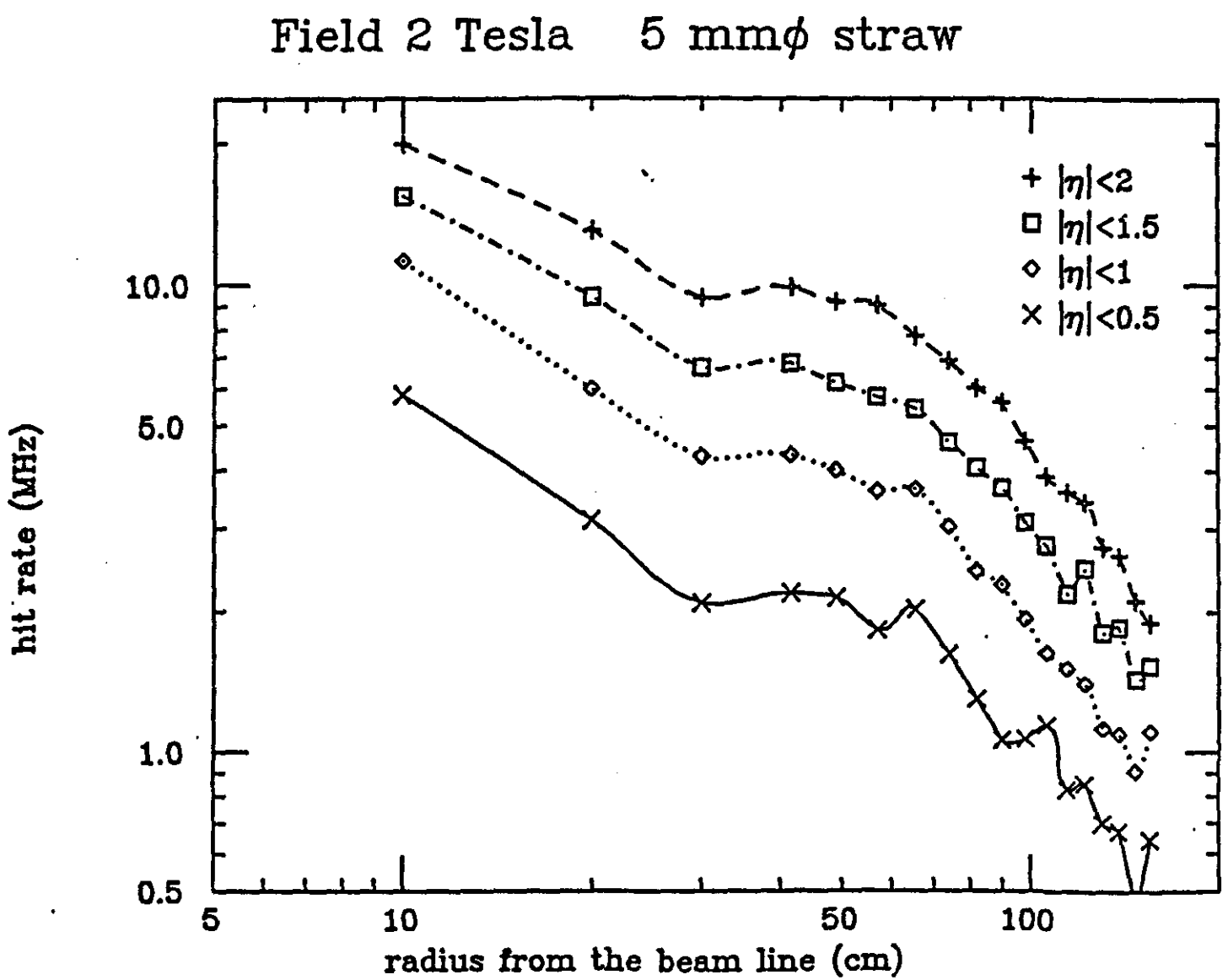
Field 2 Tesla 5 mmϕ straw
+ |η|<2
□ |η|<1.5
◇ |η|<1
× |η|<0.5
10.0
5.0
1.0
0.5
hit rate (MHz)
5
10
50
100
radius from the beam line (cm)

Fig. 1

CONCEPTUAL DESIGN OF CENTRAL TRACKING DEVICE

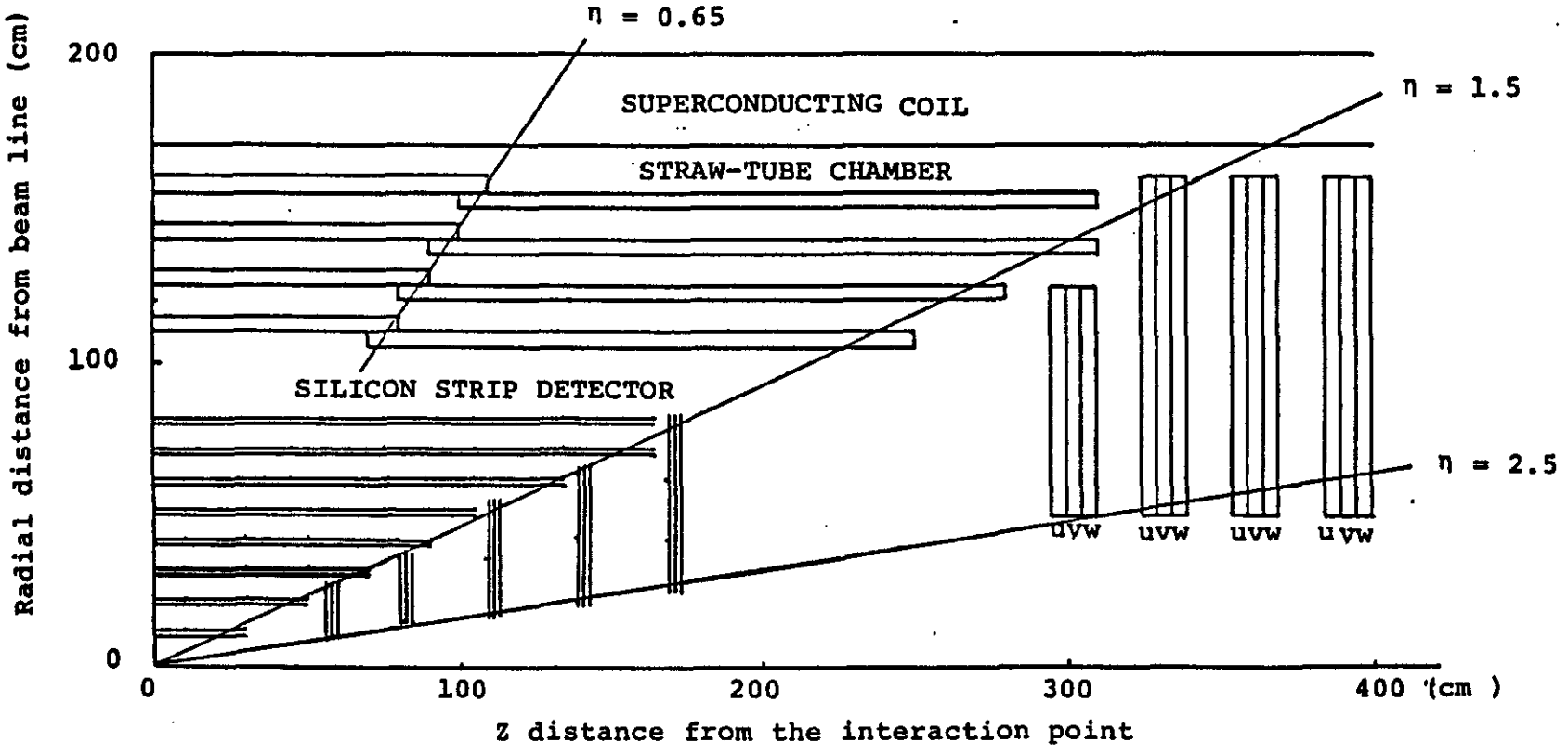

Fig. 1

SCHEMATIC VIEW OF UNIT DETECTOR

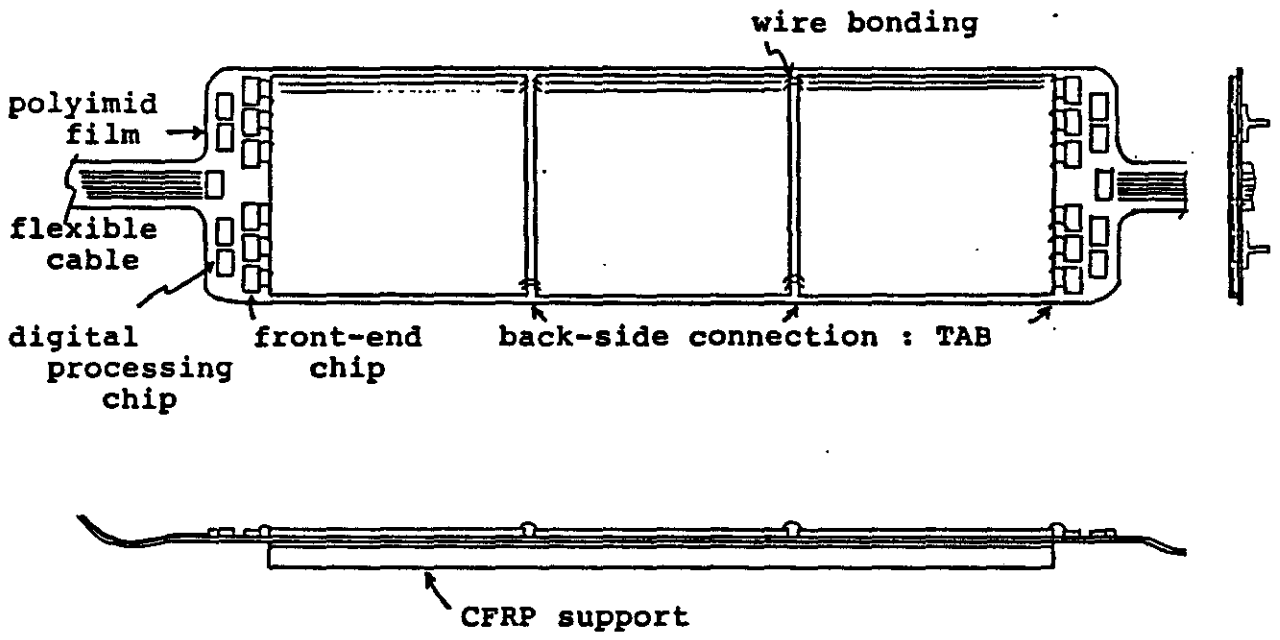

Fig. 4

CRACKLESS INTEGRATION SCHEME

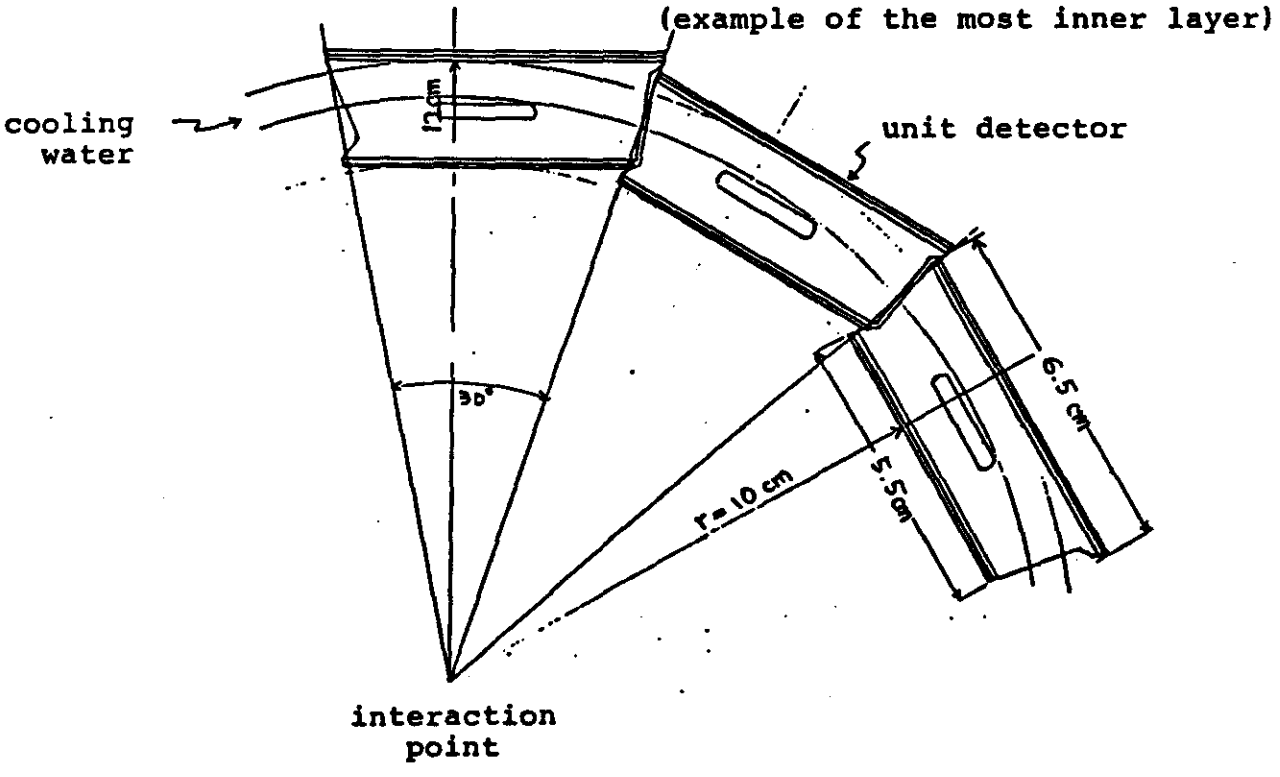

Fig. 5

SCHEMATIC VIEW OF ENDCAP
STRAW-TUBE CHAMBER TRACKING SYSTEM

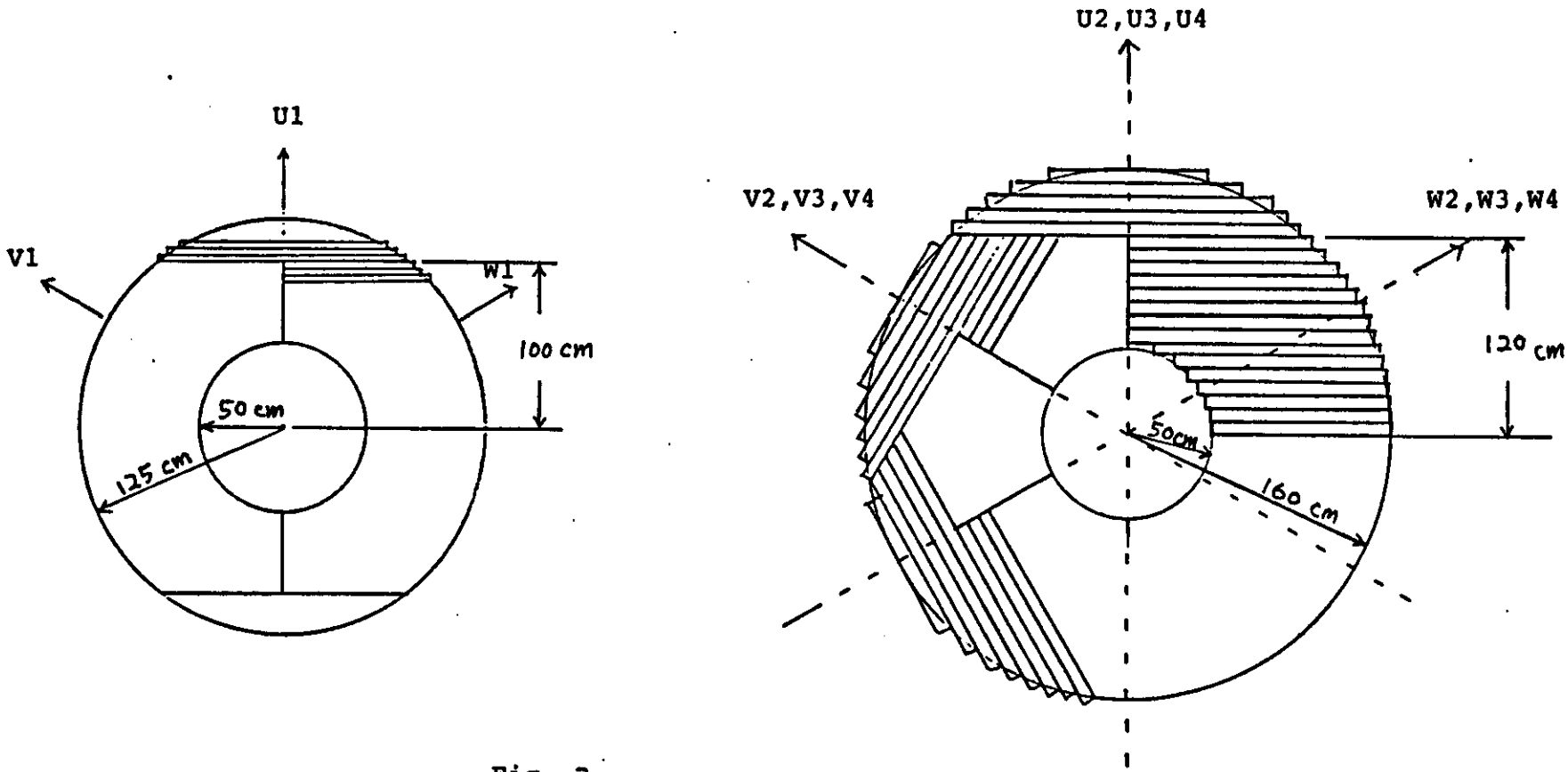

Fig. 8

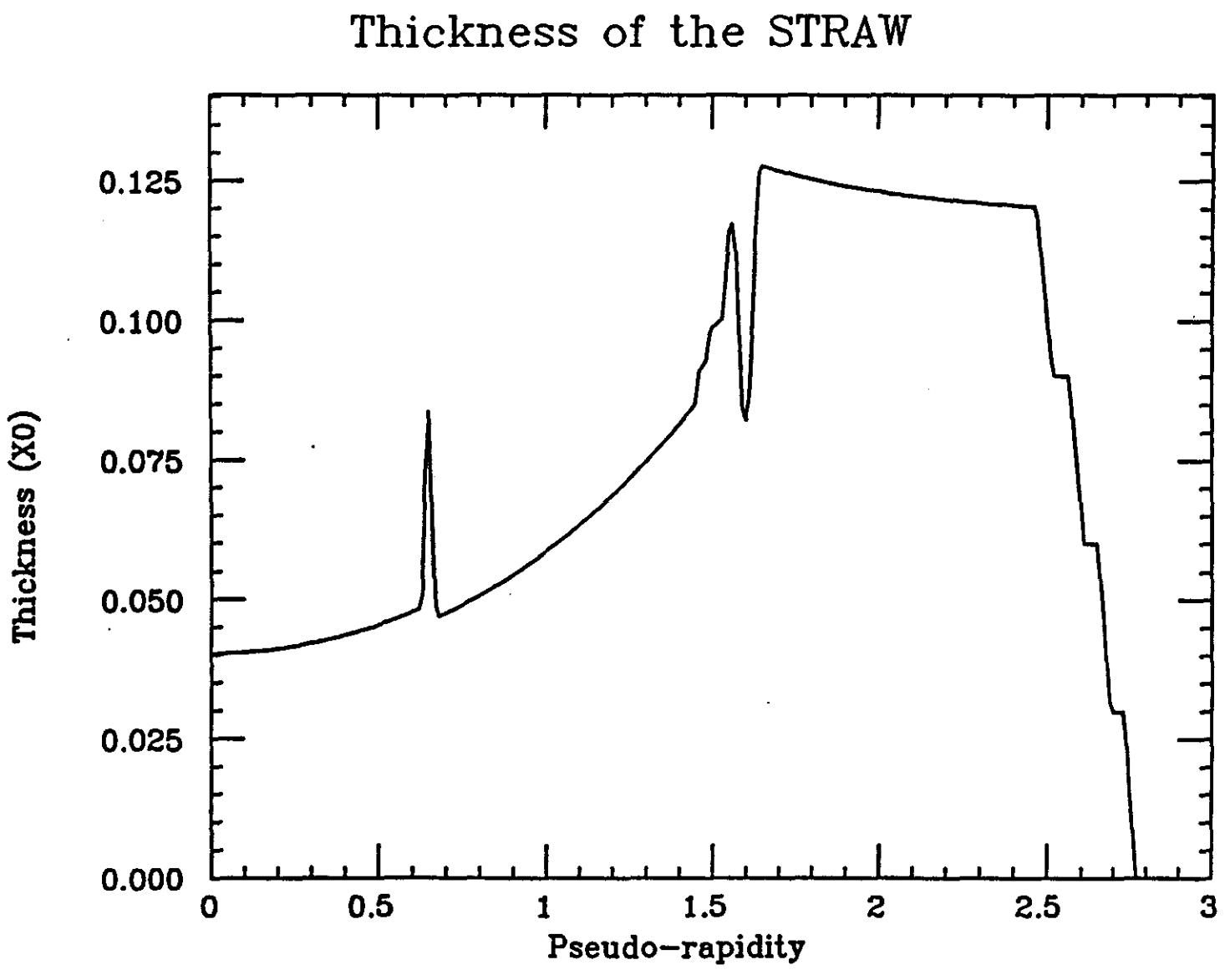
Thickness of the STRAW
Thickness (X0)
0.125
0.100
0.075
0.050
0.025
0.000
0
0.5
1
1.5
2
2.5
3
Pseudo-rapidity

Fig. 7-a

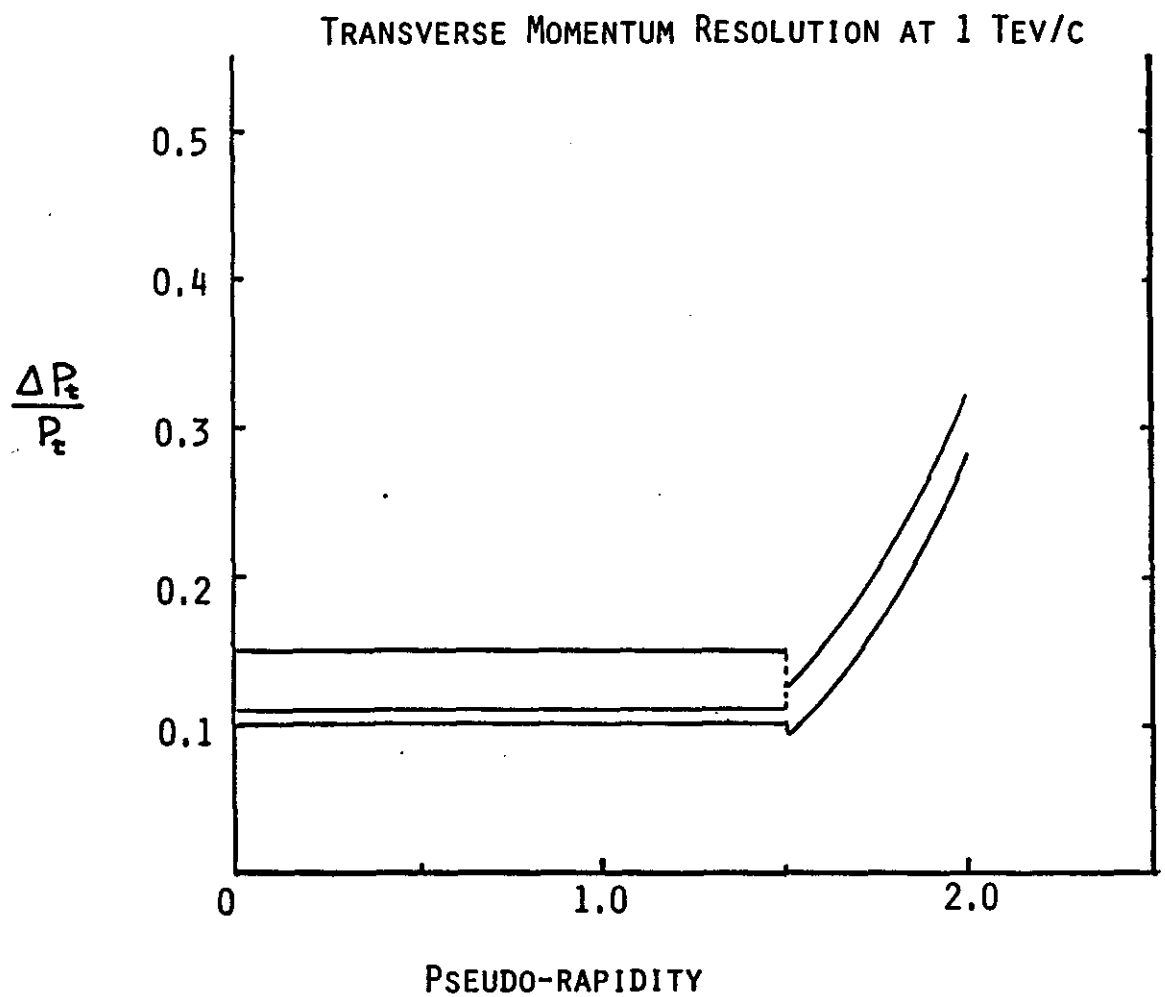
TRANSVERSE MOMENTUM RESOLUTION AT 1 TEV/C
0.5
0.4
0.3
0.2
0.1
$\frac{\Delta P_t}{P_t}$
0
1.0
2.0
PSEUDO-RAPIDITY

FIG. 6